Bulg. J. Phys. **34** (2007) 1–16

Phase Analysis of Fe-Nanowires Encapsulated into Multi-Walled Carbon Nanotubes via ^{57}Fe Mössbauer Spectroscopy

T. Ruskov[1], **I. Spirov**[1], **M. Ritschel**[2], **C. Müller**[2], **A. Leonhardt**[2], **R. Ruskov**[3]

[1]Institute for Nuclear Research and Nuclear Energy, Bulgarian Academy of Sciences, Tsarigradsko Chaussee 72, BG-1784, Sofia, Bulgaria

[2]IFW Dresden, Leibnitz Institute of Solid State and Materials Research Dresden, Helmholtzstrasse 20, D-01069 Dresden, Germany

[3]The Pennsylvania State University, Physics Department, University Park, PA 16802, USA

Received *5 January 2007*

Abstract. We have performed morphological analysis of samples of Fe-nanowires encapsulated into aligned multi-walled carbon nanotubes (Fe-MWCNT) via ^{57}Fe Mössbauer spectroscopy. The aligned Fe-MWCNTs were obtained by pyrolysis of ferrocene onto an oxidized Si substrate. Transmission Mössbauer spectroscopy (TMS) and back scattered conversion electron Mössbauer spectroscopy (CEMS) were applied in order to distinguish different Fe phases and their spatial distribution within the whole sample and along the tubes' height. A characterization (on a large spatial scale) of the aligned CNT samples were performed by obtaining TMS spectra for selected spots positioned at different locations of the sample. While the total Fe content changes considerably from one location to another, the γ-Fe/α-Fe phase ratio is constant onto a relatively large area. Using TMS and CEMS for all aligned Fe-MWCNTs samples it is also shown that along the CNT axes, going to the top of the nanotube the relative content of the γ-Fe phase increases. Going to the opposite direction, i.e. towards the silicon substrate, the relative content of the Fe_3C phase increases, that is in agreement with our previous works. The results of an additional Mössbauer spectroscopy experiment in TMS and CEMS modes performed on a non-aligned sample support the conclusion that in our case the iron phases in the channels of carbon nanotubes are spatially separated as individual nanoparticles. The relative intensity ratio of the α-Fe phase Mössbauer sextets show good magnetic texture along nanotubes axis for one of the aligned samples and the lack of such orientation for the others.

PACS number: 81.07.-b, 81.16.Ta

1 Introduction

The Mössbauer effect is observed in many isotopes, but ^{57}Fe of course is the most significant one. The reason is the smallness of the width of the resonance γ-lines in the Mössbauer spectra compared to the characteristic energies of hyperfine interaction of ^{57}Fe nucleus with their surrounding electrons. Besides that the resonant cross section is 200 times greater than that of photoelectric absorption. The resonant absorption of 14.41 keV resonant line can dominate even iron is a minor constituent of the sample. In addition Fe is an element of great commercial importance.

Fe-filled multi-walled carbon nanotubes (Fe-MWCNT) may be considered as magnetic nanowires encapsulated in thin carbon shells [1-8]. They are investigated from different points of view: preparation conditions [4], structural properties [1-4,7], magnetic properties [2,3,5,8]. The Fe-MWCNTs promise to be a good candidate for new instruments [6], for example, as sensors for magnetic scanning probe microscopy [9], for spintronics devices [10,11], high-density magnetic memory materials etc. An important problem to be resolved is in what phases (structural, magnetic, etc.) Fe exists inside the nanotubes and what is their spatial distribution. Investigations in this direction will provide information on the process of Fe-nanotubes growth and also will be important for future applications.

Different methods have been applied for the studies of Fe-MWCNTs, such as X-ray diffraction (XRD), selected area electron diffraction (SAED), scanning electron microscopy (SEM), transmission electron microscopy (TEM), high resolution transmission electron microscopy (HRTEM), alternating gradient magnetometry (AGM) measurements, ^{57}Fe Mössbauer spectroscopy. The results and conclusions about the spatial distribution and content of the Fe phases sometimes were controversial [2,3,5,7,8] and therefore need further clarification.

In this paper a ^{57}Fe transmission Mössbauer spectroscopy (TMS) and a back scattered conversion electron Mössbauer spectroscopy (CEMS) were applied in order to distinguish different Fe phases and their spatial distribution on aligned nanotubes samples. The samples were obtained by pyrolisis of ferrocene onto an oxidized Si substrate at various growth conditions. Complementary characterization of the Fe-MWCNTs was performed using X-ray diffraction (XRD), scanning electron microscopy (SEM), transmission electron microscopy (TEM), and high resolution transmission electron microscopy (HRTEM). The Mössbauer measurements reveal a large scale (on the order of mm) spatial distribution along the Si substrate and a distribution along the tubes' height as well that is consistent with the growth conditions. We performed additional Mössbauer measurements on specially prepared non-aligned samples that used the depth selective capabilities of CEMS and allowed us to conclude that in our case each of the Fe phases inside the tubes exists as separate nanoparticle. In some samples we observed

well established magnetic texture correlated with the strong shape anisotropy along the tube's axis.

2 Experimental

The multi-walled Fe-filled CNTs were grown in a quartz tube reactor inside a dual zone furnace system. The main parameters of the deposition process are the sublimation temperature of the ferrocene ($T_1 = 155°$C) in the first furnace zone, the gas flow rate of Ar or Ar/H_2 mixture, about 120–180 sccm (standard cubic centimeter per minute), and the deposition temperature in the second furnace zone ($T_2 = 860°$C for samples FN71-76 and $T_2 = 830°$C for sample 41f) where the pyrolysis of ferrocene and the deposition of filled tubes take place [4]. Thermally oxidized silicon plate with thickness 275 μm coated with 2 nm layer of Fe, or Permaloy (py) were used as substrates. The nanotubes were formed on silicon substrates placed inside the reaction zone and in this case they were aligned perpendicular to the substrate surface. Much more nanotubes were formed on the wall of the quartz tube reactor (as a mixture of bundles of well-aligned Fe-filled MWCNTs). The dimensions of both kind of nanotubes – the lengths, the core diameter, and the shell diameter were measured directly by SEM, TEM and HRTEM. The preparation conditions and a range of dimension characteristics of the Fe-MWCNTs are presented in Table 1.

Table 1. Preparation conditions and characteristics of aligned Fe-MWCNT samples.

Sample	Substrate	Growth temperature (°C)	Growth time (min)	Length (μm)	d (inner/outer) (nm)
FN71	Si/SiO_2/2nmpy	860	146	up to 30	3.5-25/8-60
FN72	Si/SiO_2/2nmpy	860	121		
FN76	Si/SiO_2/2nmpy	860	139		
41f	Si/SiO_2/2nmFe	830	5	4	5-20/10-80

^{57}Fe Mössbauer spectroscopy measurements have been performed on two types of Fe-containing MWCNTs samples: (1) samples of Fe-MWCNTs aligned perpendicularly to the Si substrate and (2) samples of carpet-like material, deposited on the inner wall of the quartz reactor tube. The samples of aligned Fe-MWCNTs without any additional procedures were subjected to a Mössbauer experiment both in transmission mode and in CEMS mode. The sample of carpet-like material in form of powder for the purpose of a Mössbauer transmission mode measurement was prepared by mixing the material with 1.3% polyvinyl-alcohol water solution with subsequent drying. The sample from the same material for CEMS mode was prepared as follows: On the one side of a Plexiglas disk with a diameter of 16 mm and a thickness of 1 mm a double side sticky tape was glued on it. The tape was covered by about 1 mg of the carpet-

like powder material, then pressed to keep it in tight contact with the tape and the Plexiglas disk.

Mössbauer spectra were taken with a conventional constant acceleration spectrometer at room temperature (RT). A ^{57}Co(Rh) source with a diameter of the activity spot of 2 mm was used. The conversion electron Mössbauer spectroscopy measurements were carried out with a He gas flow proportional counter [12]. All spectra were fitted using an integral Lorentzian line shape approximation [13,14]. In the case of aligned Fe-MWCNTs samples the direction of the incident gamma-ray beam coincides with the nanotubes axis, i.e. it is perpendicular to the Si substrate. The parameters of the fitted spectra corresponding to isomer

Table 2. Mössbauer parameters obtained from the fit of the spectra

Sample	Component	IS (mm/s)	QS (mm/s)	H (kOe)	Relative area (%)
FN71 transmission	α-Fe	0.002±0.004	0.005±0.004	333.7 ±0.3	70± 0.9
	Fe_3C	–	–	–	–
	γ-Fe	-0.11± 0.01	–	–	30± 0.9
FN72 transmission	α-Fe	0.00 ± 0.01	0.01± 0.02	332.3±0.6	62 ± 2
	Fe_3C	0.2 ± 0.1	0.07± 0.2	205±6	6 ± 2
	γ-Fe	-0.10 ± 0.02	–	–	32 ± 2
FN72 CEMS	α-Fe	-0.004± 0.007	0.00 ± 0.01	331.8±0.5	59 ± 1
	Fe_3C	–	–	–	–
	γ-Fe	-0.100.01	–	–	41 ± 1
FN76 transmission	α-Fe	-0.001±0.007	0.00±0.01	334.7±0.4	69 ± 1
	Fe_3C	0.20 ± 0.06	0.0± 0.1	211±4	8 ± 1
	γ-Fe	-0.11 ± 0.02	–	–	23 ± 1
FN76 CEMS	α-Fe	0.00±0.01	0.00±0.02	330.5±0.5	75 ± 2
	Fe_3C	–	–	–	–
	γ-Fe	-0.09± 0.03	–	–	25 ± 2
Powder transmission	α-Fe	0.003±0.002	0.015±0.003	331.5±0.2	83.6 ± 0.5
	Fe_3C	0.23± 0.02	0.07± 0.03	206±1	9.3 ± 0.5
	γ-Fe	-0.12± 0.02	–	–	7.2 ± 0.5
Powder CEMS	α-Fe	-0.003±0.004	0.021±0.006	330.3±0.3	84 ± 1
	Fe_3C	0.18± 0.04	0.03± 0.06	209±3	7 ± 1
	γ-Fe	-0.09± 0.04	–	–	9 ± 1
41f CEMS	α-Fe	-0.012± 0.02	0.00±0.02	328±1	56 ± 2
	Fe_3C	–	–	–	–
	γ-Fe	-0.093± 0.02	–	–	44 ± 2

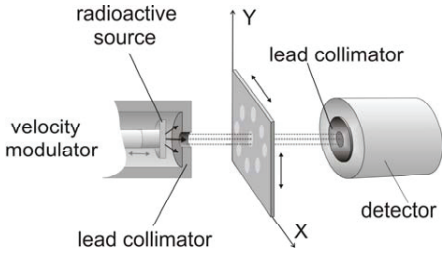

Figure 1. Transmission Mössbauer spectroscopy setup for measuring morphology of aligned Fe-MWCNT samples.

shift (IS), quadrupole shift (QS), magnetic field at the site of the Fe nucleus (H), and the relative spectral areas are shown in Table 2. The isomer shifts of the spectra are referred to the centroid of an α-Fe foil reference spectrum at room temperature. The geometric effect due to the source motion is taken into account as well.

To measure the morphology of aligned Fe-MWCNTs along the substrate the samples were mounted on a two-axis (X, Y)-travelling microscope stage that controls the position of the sample with respect to the collimated gamma-ray beam by two micrometer screws (Figure 1). Nine different positions of the sample that correspond to nine irradiated spots were chosen as is shown in the figure. The diameter of each irradiated spot was 3 mm. By means of that setup two aligned Fe-MWCNTs samples 20×20 mm^2 (FN 71 and FN 72) were scanned using ^{57}Fe transmission Mössbauer spectroscopy mode.

In ^{57}Fe conversion electron Mössbauer spectroscopy the detection of back-scattered conversion electrons is used for the study of the surface and layers in the immediate vicinity of the surface, In our experiments we used a gas flow proportional counter, in which case large counting rates can be obtained (Figure 2). Although the energy resolution of proportional counter is poorer than that of vacuum electron spectrometers, it is sufficient for a rough separation of

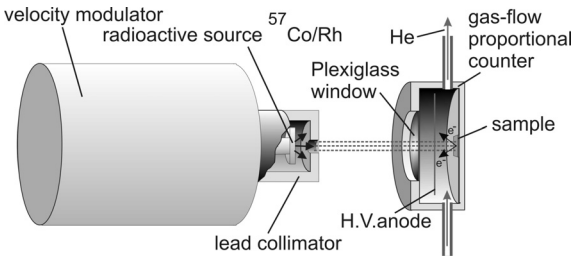

Figure 2. Conversion electron Mössbauer spectroscopy setup with gas flow proportional counter.

the conversion electrons emitted by the surface from the electrons emitted by deeper layers.

3 Experimental Results and Discussion

3.1 Preliminary Characterisation

Figure 3a and Figure 3b show SEM images for two of the samples, 41f and FN 76, respectively. It is seen that the nanotubes of sample 41f grown onto the Si substrate exhibit a distinct alignment perpendicular to the substrate surface (Figure 3a), while in the case of the FN 76 sample many branched tubes and tubes with an alignment not perpendicular to the substrate are observed. We have to mention that close to the substrate (at the beginning of deposition) the alignment of nanotubes for FN 76 sample is better, but after 9–10 μm deposition the alignment is strongly distorted. The main difference in preparation conditions for the samples mentioned above (Table 1) is the growth time: 5 min for the 41f sample and 139 min for the FN 76 sample, leading not only to different

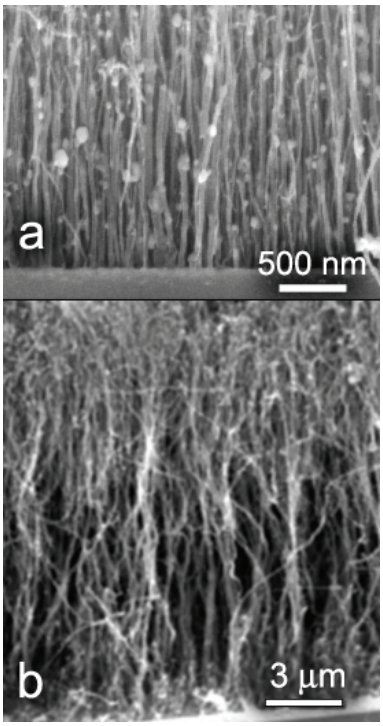

Figure 3. SEM images for samples: (a) 41f and (b) FN 76.

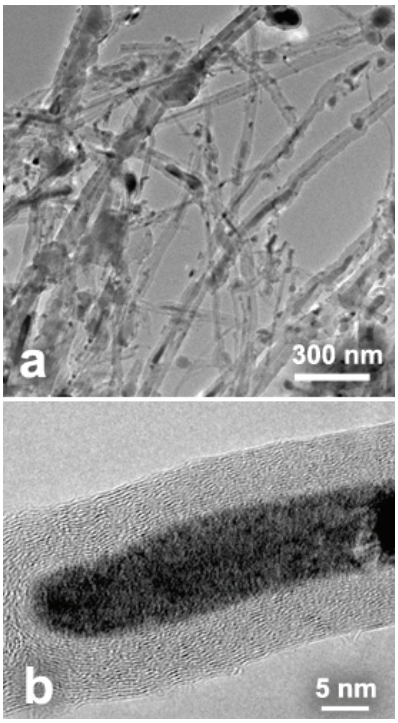

Figure 4. (a) TEM image for sample 41f and (b) HRTEM image for sample FN 76.

length of the nanotubes (4 μm, and approximately 30 μm, respectively), but also to different quality of alignment. In Figures 4a and 4b TEM images of the 41f and FN 76 samples are shown as well. The TEM image, Figure 4a, shows that the tubes are filled with a chain of iron particles of different shapes. The HRTEM image, Figure 4b, shows the edge of one Fe-filled MWCNT of the FN 76 sample. One can see the walls of the tube consisting of cylindrically curved graphite lattice shells parallel to the tube axis closing at the edge of the tube.

3.2 Mössbauer Spectroscopy Analysis

A. Large scale morphology along the substrate

Figure 5 shows the results of scanning *via* TMS of the selected spots of aligned Fe-MWCNTs samples that reveal their morphology. A typical transmission

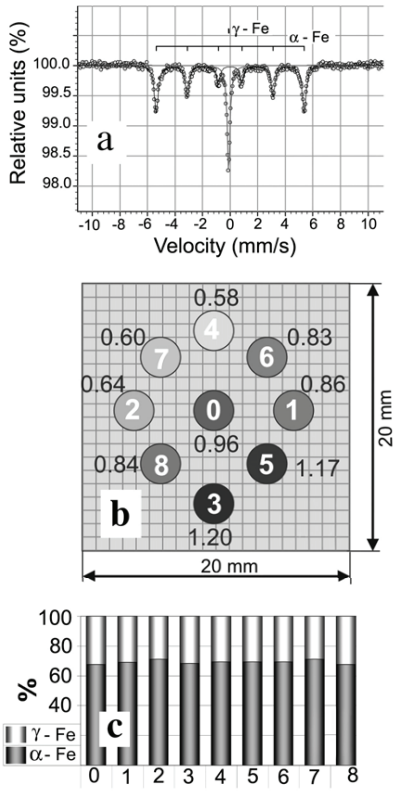

Figure 5. The result of Mössbauer spectroscopy scanning of aligned Fe-MWCNT samples: (a) typical Mössbauer spectrum of the sample FN 71, (b) relative content of the deposited iron (γ-Fe + α-Fe) in the nanotubes at nine different positions, and (c) γ-Fe – α-Fe percentage content for the same nine positions.

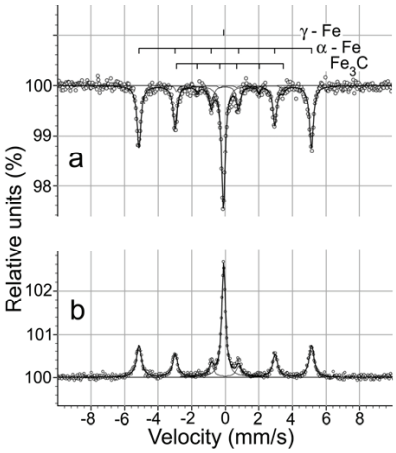

Figure 6. Mössbauer spectra of aligned Fe-filled MWCNT sample FN 72: (a) transmission mode; (b) CEMS mode.

Mössbauer spectrum, which corresponds to the FN 71 sample, is shown in Figure 5a. Only two iron phases exhibit in the spectrum: the ferromagnetic α-Fe (bcc) and the paramagnetic γ-Fe (fcc). In Figure 5b we give the relative content of the deposited iron (γ-Fe + α-Fe) in the nanotubes, that is determined from the measured areas of Mössbauer spectra for nine different positions of the sample. The corresponding partial content of the phases for the same nine positions is presented in Figure 5c. While the total iron content changes from position to position (within 10–30%), the phase ratio for these nine positions remains almost the same (within 1–2%). In other words, there is relatively good homogeneity with respect to the phase ratio but not with respect to the total iron content.

A plausible explanation for this phenomenon may be the following. The tube-length decreases from the front to the backside of the substrate (along the gas flow direction); and correspondingly the total iron content decreases. It is in correspondence with the observation that in the horizontal CVD-reactor there exists a concentration gradient of ferrocene over the substrate, from the front to the backside, and thus a ferrocene depletion. On the other hand, the phase ratio is primarily dependent on the deposition temperature and it is approximately constant about the whole deposition location. We also note in passing, that the inhomogeneity of the deposited iron may become possible simply due to different density of the CNTs that grow on the silicon substrate (in the sense of nonuniform distance between the CNTs). In addition, there might be some distribution of the inner CNT diameters (due to the change of the catalyst-particle size) in the Si substrate plane.

Which iron phases are deposited into the CNT channels during the pyrolysis of ferrocene and what is their ratio, depends on the preparation conditions. In gen-

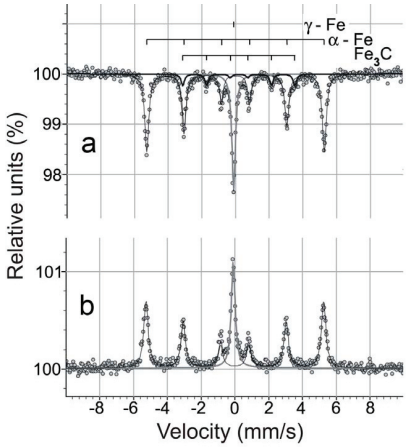

Figure 7. Mössbauer spectra of Fe-filled MWCNT sample FN 76: (a) transmission mode; (b) CEMS mode.

eral, three phases are observed: α-Fe, γ-Fe, and Fe_3C. However, the Fe_3C phase is absent in the sample FN 71, as seen in Figure 5a, while all three phases are present in the samples FN 72 (Figure 6a) and FN 76 (Figure 7a). We noted that the preparation conditions for nanotubes growth in the samples FN 71, FN 72, and FN 76 are almost the same, namely: the temperature in the first furnace zone is $T_1 = 155^{\circ}$C, while for the second one it is $T_2 = 860^{\circ}$C; the velocity of Ar flow in the quartz reactor tube is 180 sccm, and only the deposition time is varied between 121 min (FN 72) and 146 min (FN 71) respectively. The samples' cooling rate was also identical for all samples (20°C per minute). The absence of the iron carbide phase in the case of sample FN 71 is not absolutely clear. Perhaps the longer deposition time means a longer annealing of the filling material that eventually leads to a decomposition of the thermodynamically unstable Fe_3C to iron and graphite [8].

B. Along the tubes' height morphology

Another interesting question concerns the spatial distribution of the Fe phases inside the nanotube channels that received different opinions in the literature [2,3,5,7,8]. Our approach of simultaneous application of ^{57}Fe transmission Mössbauer spectroscopy (TMS) and back scattered conversion electron Mössbauer spectroscopy (CEMS) for the same sample allows us to obtain additional information for the spatial distribution of the Fe phases. Indeed, the TMS provides information from the "bulk" of the sample, while the CEMS provides information from the surface layer or from layers in the immediate vicinity to the surface. It is well known for the conversion electrons methods that after

a resonance absorption of gamma-quanta in the sample, the main contribution to the resonance spectrum comes from the emitted K-shell conversion electrons with energy 7.3 keV with a subsequent emitting of Auger electrons with energy of 5.4 keV. These electrons can escape from a layer with thickness of the order of 100–200 nm (actually 90% come from a layer with thickness of the order of 100 nm [12]); the estimation is for pure iron. Since the distance between the nanotubes of the aligned samples is of the order or even larger than the average nanotube diameter, it should be expected that the effective thickness of the top layer is actually somewhat larger than the above estimation because some of the conversion electrons may escape through the inter-tube space.

The transmission Mössbauer spectrum of the sample FN 72 (Figure 6a) as compared to that of the sample FN 71 shows an appearance of a third iron phase (Fe_3C) and the corresponding phase ratio α-Fe : Fe_3C : γ-Fe is 62%: 6% : 32%. The spectrum measured in the CEMS mode (Figure 6b) for the same iron phases gives 59% : 0% : 41% (Table 2). Thus, one observes a 9% increasing of the γ-Fe and absence of Fe_3C in the top layer of this sample of aligned Fe-MWCNTs. Similar change in the phase content as observed in the conversion spectrum with respect to the corresponding transmission spectrum is derived for the sample FN 76 from Figure 7 and Table 2. Here Figure 7a shows the Mössbauer spectrum in the transmission mode, and Figure 7b shows the spectrum in the CEMS mode. Again, in the transmission mode we see all three phases: α-Fe, γ-Fe, and the well established iron carbide phase. In the CEMS mode we observe a small increase of the γ-Fe and α-Fe and also a total diminishing of the iron carbide.

We mention that the increase of relative content of γ-Fe in the top layer has been observed by us in all aligned samples reaching in some of them the limiting case when only the γ-Fe phase is present [7]. On the other hand, we observe that the Fe_3C phase is diminished to zero in the top layer (or correspondingly, it could be said to increase towards the silicon substrate). These results show a spatial distribution of the Fe phases along the height of the nanotubes which is in agreement with the work of Leonhardt *et al.* [8]. In that work the authors have investigated aligned Fe-MWCNTs on a silicon substrate, which were obtained by the same method of pyrolysis of ferrocene, mentioned above. In their work the samples were examined by means of an X-ray diffraction method at different glancing angles of the X-ray beam with respect to the silicon substrate plane. While qualitatively, the authors from Ref. [8] show that at small glancing angles (0.5° and 1°) the intensity of the diffraction γ-Fe peaks increases with respect to analogous peaks for a diffraction pattern at a glancing angle of 5°, they also mention that at larger glancing angles one observes an increase of the diffraction peaks corresponding to Fe_3C.

The observed spatial distribution of the different Fe phases along the height of the aligned nanotube samples can be explained qualitatively with the temperature gradient during the cooling process that is applied in the hot furnace zone of the quartz reactor tube, after the pyrolysis of ferrocene and the growth of the

Fe-filled nanotubes. The γ-Fe or a mixture of γ-Fe and iron carbide are the existing phases according to the phase diagram Fe-C at a temperature of 860°C and up to 6.5 weight % of carbon. At the cooling process below the eutectic temperature (738°C), the γ-Fe transforms to α-Fe and Fe_3C. This transformation is the stronger the slower the cooling process. At a cooling process that uses an Ar flow (the rector heater is switched off) the cooling at the top layer is more effective compared to the bulk (or to the interface range tubes-substrate). Therefore, the observed phases on the top layer of the nanotube samples show an incomplete transformation of the γ-Fe to α-Fe and Fe_3C (that is, the phase state is "frozen" as compared to that near the substrate).

C. More arguments about the distribution of iron phases inside the MWCNTs

The question of spatial distribution of the iron phases inside the MWCNTs channels was also addressed in the works of Prados *et al.* [2] and Marco *et al.* [3]. Based on combined transmission Mössbauer spectroscopy and magnetic measurements in the temperature range of 4.2–300 K, the authors of those works have reached to the conclusion that the channels of the nanotubes are filled with axially elongated nanoparticles containing iron. The spatial distribution of the iron phases is conjectured so that the core of every particle is of α-Fe, surrounded by a layer of γ-Fe, and finally surrounded by an interface layer of Fe_3C; the last being in contact with the inner CNT shell. In other words, all three iron phases are present in any of the nanoparticles according to their model.

However, the results of our paper as well as our previous results [7] show that in our samples such a model is far from reality. Indeed, the method of transmission Mössbauer spectroscopy by itself cannot provide information about the spatial distribution of iron phases. The conclusion in Refs. [2,3] is based mainly on magnetic measurements, and especially on the observed shift of the magnetic hysteresis loop when the sample under an external magnetic field was cooled below the point of phase transition from paramagnetic to antiferromagnetic state of the γ-Fe phase. In general, it is known that such shift of the hysteresis loop can be explained by an α-Fe/γ-Fe exchange coupling. According to the authors, there should be a common contact surface between the α-Fe and γ-Fe, which is the main reason for their model of spatial distribution of the iron-containing phases.

It is worth to mention, that magnetic measurements of different types of Fe-filled nanotubes obtained by the Dresden group by pyrolysis of ferrocene do not show a shift of the hysteresis loop within the accuracy of 2 Oersteds [5]. This means that an α-Fe/γ-Fe exchange coupling, if any, is negligible in our case. In addition, our investigation of individual CNTs, by means of the selected area electron diffraction (SAED) analysis [7] has revealed that the nanotubes contain single crystals grains having either the bcc (α-Fe) or fcc (γ-Fe) structure.

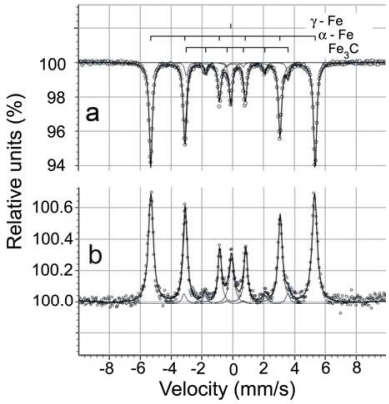

Figure 8. Mössbauer spectra of carpet-like material, taken from the reactor walls: (a) transmission mode; (b) CEMS mode.

Another investigation also at RT of individual CNTs using electron holography show that the tubes are filled with a chain of iron particles of different shapes; part of them being in ferromagnetic and another part in paramagnetic state [5].

In order to further clarify this point, we have performed additional Mössbauer measurements with a sample prepared from the carpet-like material, in the form of powder, taken from bundles of aligned MWCNTs deposited on the inner wall of the quartz reactor tube. Figure 8 shows two Mössbauer spectra for this material, one of them is obtained in the transmission mode (Figure 8a) and the other in the CEMS mode (Figure 8b). In both spectra we observed the three phases: α-Fe, γ-Fe, and Fe_3C. More important is that both Mössbauer spectra show the same relative content of the three phases within the experimental accuracy. This experimental result is in accordance with our model of spatial distribution, in which iron phases are considered as individual particles, in the channels of the carbon nanotubes. The difference between the spectra in the two modes observed previously for the aligned samples should not be seen in this experiment since the nanotubes in the powder samples are randomly oriented and one cannot distinguish "top" and "bottom" of the nanotube. (The random orientation is supported by the relative ratio of the intensities of 3:2:1:1:2:3 of the α-Fe sextet, as seen in Figure 8a).

If, however, we would accept the model of composite nanoparticles (α-Fe/γ-Fe/Fe_3C) of Prados *et al.* [2,3], there should be an observable difference between the relative contribution of iron phases in the two spectra. Let us explain this statement. Due to multiple scattering and self-absorption of emitted conversion electrons in the nanotubes, the energy of conversion electrons is spread from zero to 7.3 keV. It is obvious that the higher the energy of conversion electrons the more close to the surface they are emitted. Although the energy

resolution of a proportional counter is much poorer than that of vacuum electron spectrometers, choosing the window of the single-channel analyser to the highest-energy part of the conversion electron pulse-height spectrum a separation of the conversion electrons emitted by the layers in the immediate vicinity of the surface from the electrons emitted by deeper layers is possible [12]. We have to mention that the main self-absorption will take place in the iron core of the Fe-filled nanotubes because the density of iron is approximately four times larger than that of carbon. The nanotubes in the powder samples have a core diameter in the range of 30–40 nm. The thickness of graphite walls is of the same order. By cutting appropriately the low-energy part of the conversion electron spectrum in the pulse height spectrum of the proportional counter, we are able to register only the electrons that come from a surface layer with *a thickness of the order of the average nanotube radius*. If the model of Prados *et al.* [2,3] would be correct one could expect some *decreasing of the α-Fe spectral area*, S_α, in the CEMS spectrum and increasing of the γ-Fe and Fe_3C spectral areas, $S_{\gamma+C}$, comparative to the transmission spectrum. Thus, overall, the ratio $R_S \equiv S_{\gamma+C}/S_\alpha$ *should increase*. The main reason is that the α-Fe core is farther to the nanotube surface and the electron self-absorption will be higher for this iron phase according to the accepted model. On the other hand the γ-Fe and Fe_3C phases are closer to the surface and therefore the self-absorption for these electrons should be smaller, which should affect the relative spectral areas in the CEMS mode. Very rough estimations based on simplified geometry and an exponential attenuation of emitted conversion electrons show that the relative change of the ratio, $\Delta[R_S]/R_S$, in our case would be about 60–70%, while it would be smaller (about 10%) if we did not cut the low energy part of the pulse-height spectrum. However, we did not observe any changes concerning the spectral area ratio, $S_{\gamma+C}/S_\alpha$, in the CEMS spectrum.

Summarizing the results of the ^{57}Fe Mössbauer spectroscopy measurements and the results of other measurements mentioned above we can make the conclusion that in our case the iron phases in the channels of carbon nanotubes are spatially separated as individual nanoparticles, while a model of compound nanoparticles, proposed in Refs. [2,3] is excluded by our experiment. It would be interesting to clarify, however, what is the reason for such considerable differences as to the results of hysteresis magnetic measurements obtained by Mühl *et al.* [5] and those described in the works [2,3].

D. Magnetic texture

In addition to the above spatial morphology analysis we report here some new data on the magnetic texture of the Fe-MWCNTs obtained via Mössbauer spectroscopy. It is well known that from the relative intensities of the six resonance lines for a given ferromagnetic phase it can be deduced what is the orientation of the magnetization axis of this phase with respect to the direction of the gamma

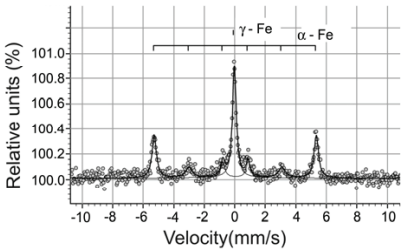

Figure 9. CEM spectrum of aligned Fe-filled MWCNT sample 41f.

rays. If the two directions coincide exactly, i.e., the angle between the magnetic moment of this phase and the direction of the gamma-quanta is zero or 180 degrees, then the ratio of the intensities of the sextet should be 3:0:1:1:0:3. In case of perpendicular orientation the intensity ratio should be 3:4:1:1:4:3. For a multi-domain structure and if the ferromagnetic domains in the nanotubes are oriented randomly, or if the carbon nanotubes in the sample are oriented randomly, the relative intensities of the six lines follow the ratio 3:2:1:1:2:3 [15,16].

As mentioned above, in the case of aligned Fe-MWCNT samples the direction of the incident gamma-ray beam coincides with the nanotube's axis. Therefore, from the intensity ratio for the ferromagnetic phase we can obtain information about its magnetic texture. Figure 9 shows a Mössbauer spectrum of the aligned Fe-MWCNT sample 41f in CEMS mode. Spectrum in the transmission mode is not presented since the length of the nanotubes is relatively small and the amount of deposited iron is too small to be detectable with good statistics in this mode. The relative intensities of the six lines for the ferromagnetic α-Fe follow a ratio 3:0.7:1:1:0.7:3. This is a clear signature that there is a comparatively good orientation of the remanent magnetization along the axis of the aligned nanotubes. It is connected with an anisotropy of the form in such magnetic nanowires, in which the magnetic easy axis coincides with the nanotubes' axis. It is known from the Mössbauer spectroscopy experiments with α-Fe nanowires obtained by electrodeposition in porous aluminium oxide templates that the smaller diameter of α-Fe nanowires the stronger magnetic texture could be obtained [17]. For instance, according to the results [17], α-Fe-nanowires with diameter below 50 nm and length 5 μm show very good orientation of magnetic moment along the nanowire axis. In our case, the nanotubes' core diameter of sample 41f is 5–20 nm and the length is 4 μm (Table 1). On the other hand, the relative intensities of the six lines for the ferromagnetic α-Fe in FN 71, FN 72, and FN 76 samples follow a ratio 3:2:1:1:2:3, although the nanotubes' core diameter is of the same order (3.5–25 nm). However, the length in that case is 30 μm and the explanation of such ratio should be connected with the strong and random distortion of the alignment of the nanotubes when their length exceeds several microns (see Figure 3b).

From the point of view of searching for new fundamental properties in mag-

netic materials, it is worth to mention that we approach the so-called *quasi-one-dimensional ferromagnetism* for the α-Fe phase. It is interesting also to answer the question what will be the critical nanotube inner diameter below which the α-Fe phase will transform to the superparamagnetic state and also what is the temperature dependence of this magnetic phase transition.

We conclude this section by mentioning, in addition, the high stability of the iron phase content of the Fe-nanowires encapsulated into the channels of the multi-wall carbon nanotubes with respect to time passing. For example, the Mössbauer spectra for the sample of carpet-like material obtained now and about two years ago have given the same iron phase content within the statistical experimental error. The inspected samples were kept without any special measures, and subjected to general changes of the temperature and moisture in the lab. It is worth to compare our result with analogous CEMS results from Ref. [17], where a presence of superparamagnetic iron oxide at the "top layer" of as deposited nanowires has been observed. This means that the carbon shell preserves very well against any corrosion processes and other possible phase changes in the encapsulated iron.

4 Conclusion

In this paper we have presented results obtained via combined Mössbauer (TMS and CEMS) measurements and also via other additional structural investigations of Fe-filled MWCNTs. These show that onto relatively large area of aligned Fe-MWCNT samples the total Fe content changes considerably from one location to another, while the γ-Fe/α-Fe phase ratio is a constant. It is also shown that along the CNT axis, going to the top of the nanotube the relative content of the γ-Fe phase increases. Going in the opposite direction, i.e. towards the silicon substrate, increases the relative content of the Fe_3C phase.

Both combined Mössbauer investigations of the samples and additional structural investigations of the individual Fe-MWCNTs show that the spatial distribution of the different iron phases is in the form of spatially separated nanoparticles, each in its own phase. In this sense, our results do not confirm a spatial distribution of the iron phases proposed earlier by Prados *et al.* [2,3], in which the authors stated that each nanoparticle inside the MWCNT consists of an α-Fe particle core, surrounded by the shell of a γ-Fe phase and finally covered by a layer of Fe_3C, which is located at the interface between the metallic phases and the inner wall of the carbon nanotubes.

We have obtained an evidence for well established magnetic texture in some of the aligned Fe-MWCNT samples. Measurements for understanding of α-Fe phase orientation mechanism and its correlation with preparation conditions of the samples are under way.

Acknowledgments

Financial support provided by the Bulgarian Ministry of Education through Grant CECOA was gratefully acknowledged.

References

[1] N. Grobert, W.K. Hsu, Y.Q. Zhu, J.P. Hare, H.W. Kroto, D.R.M. Walton, M. Terrones, H. Terrones, Ph. Redlich, M. Rühle, R. Escudero, F. Morales (1999) *Appl. Phys. Lett.* **75** 3363.

[2] C. Prados, P. Crespo, J.M. Gonzalez, A. Hernando, J.F. Marco, R. Gancedo, N. Grobert, M. Terrones, R.M. Walton, H.W. Kroto (2002) *Phys. Rev. B* **65** 113405.

[3] J.F. Marco, J.R. Gancedo, A. Hernando, P. Crespo, C. Prados, J.M. Gonzalez, N. Grobert, M. Terrones, D.R.M. Walton, H.W. Kroto (2002) *Hyp. Inter.* **139/140** 535.

[4] A. Leonhardt, M. Ritschel, R. Kozhuharova, A. Graff, T. Mühl, R. Huhle, I. Mönch, D. Elefant, C.M. Schneider (2003) *Diam. Relat. Mater.* **12** 790.

[5] T. Mühl, D. Elefant, A. Graff, R. Kozhuharova, I. Mönch, M. Ritschel, P. Simon, S. Groudeva-Zotova, C.M. Schneider (2003) *J. Appl. Phys.* **93** 1.

[6] C.M. Schneider, B. Zhao, R. Kozhuharova, S. Groudeva-Zotova, T. Mühl, M. Ritschel, I. Mönch, H. Vinzelberg, D. Elefant, A. Graff, A. Leonhardt, J. Fink (2004) *Diam. Relat. Mater.* **13** 215.

[7] T. Ruskov, S. Asenov, I. Spirov, C. Garcia, I. Mönch, A. Graff , R. Kozhuharova, A. Leonhardt, T. Mühl, M. Ritschel, C.M. Schneider, S. Groudeva-Zotova (2004) *J. Appl. Phys.* **96** 7514.

[8] A. Leonhardt, M. Ritschel, D. Elefant, N. Mattern, K. Biedermann, H. Hampel, C. Müller, T. Germming, B. Büchner (2005) *J. Appl. Phys.* **98** 74315.

[9] H. Kuramochi, H. Akinaga, Y. Semba, N. Kijima, T. Uzumaki, M. Yasutake, A. Tanaka, H. Yokoyama (2005) *Jap. J. Appl. Phys., Part 1-Regular Papers Short Notes & Review Papers* **44** 2079-2082.

[10] K. Tsukagoshi, B.W. Alphenaar, H. Ago (1999) *Nature* **401** 572.

[11] S. Sahoo, T. Kontos, J. Furer, C. Hoffmann, M. Graber, A. Cottet, C. Schonenberger (2005) *Nature Physics (London)* **1** 99.

[12] T. Ruskov, R. Ruskov, D. Paneva, D. Lefterov (1999) *Nuclear Instruments and Methods in Physics Research B* **159** 60.

[13] G.K. Shenoy, J.M. Friedt, H. Maleta, S.L. Ruby (1974) *Mössbauer Effect Methodology* **9** 277.

[14] T.E. Cranshaw (1974) *J. Phys. E* **7** 122.

[15] G.K. Werthiem (1964) *Mössbauer effect: Principles and Applications* (Academic Press, New York and London).

[16] K. Haneda (1987) *Can. J. Phys.* **65** 1233.

[17] J.B. Wang, X.Z. Zhou, Q.F. Liu, D.S. Li, B. Li, H.P. Kunkel, G. Williams (2004) *Nanotechnology* **15** 485.